



HAL
open science

Transcorrelated selected configuration interaction in a bi-orthonormal basis and a cheap three-body correlation factor

Abdallah Ammar, Anthony Scemama, Emmanuel Giner

► To cite this version:

Abdallah Ammar, Anthony Scemama, Emmanuel Giner. Transcorrelated selected configuration interaction in a bi-orthonormal basis and a cheap three-body correlation factor. 2023. hal-04136834v1

HAL Id: hal-04136834

<https://hal.science/hal-04136834v1>

Preprint submitted on 21 Jun 2023 (v1), last revised 25 Sep 2023 (v2)

HAL is a multi-disciplinary open access archive for the deposit and dissemination of scientific research documents, whether they are published or not. The documents may come from teaching and research institutions in France or abroad, or from public or private research centers.

L'archive ouverte pluridisciplinaire **HAL**, est destinée au dépôt et à la diffusion de documents scientifiques de niveau recherche, publiés ou non, émanant des établissements d'enseignement et de recherche français ou étrangers, des laboratoires publics ou privés.

Transcorrelated selected configuration interaction in a bi-orthonormal basis and a cheap three-body correlation factor

Abdallah Ammar,^{1, a)} Anthony Scemama,¹ and Emmanuel Giner^{2, b)}

¹⁾*Laboratoire de Chimie et Physique Quantiques (UMR 5626), Université de Toulouse, CNRS, UPS, France*

²⁾*Laboratoire de Chimie Théorique, Sorbonne Université and CNRS, F-75005 Paris, France*

In this work, we develop a mathematical framework for a Selected Configuration Interaction (SCI) algorithm within a bi-orthogonal basis for transcorrelated (TC) calculations. The bi-orthogonal basis used here serves as the equivalent of the standard Hartree Fock (HF) orbitals. However, within the context of TC, it leads to distinct orbitals for the left and right vectors. Our findings indicate that the use of such a bi-orthogonal basis allows for a proper definition of the frozen core approximation. In contrast, the use of HF orbitals results in bad error cancellations for ionization potentials and atomization energies (AE). Compared to HF orbitals, the optimized bi-orthogonal basis significantly reduces the positive part of the second-order energy (PT2), thereby facilitating the use of standard extrapolation techniques of hermitian SCI. While we did not observe a significant improvement in the convergence of the SCI algorithm, this is largely due to the use in the present work of a simple three-body correlation factor introduced in a recent study. This correlation factor, which depends only on atomic parameters, eliminates the need for re-optimization of the correlation factor for molecular systems, making its use straightforward and user-friendly. Despite the simplicity of this correlation factor, we were able to achieve accurate results on the AE of a series of 14 molecules in a triple-zeta basis. We also successfully broke a double bond until the full dissociation limit while maintaining the size consistency property. This work thus demonstrates the potential of the BiO-TC-SCI approach in handling complex molecular systems.

I. INTRODUCTION

In the expansive field of electronic structure calculations, the Transcorrelated (TC) method [1](#) offers an appealing path toward an accurate description of atomic and molecular systems. The TC framework uses a linear combination of Slater determinants multiplied by a correlation factor, thus enabling the inclusion of correlation effects with both real space space and orbital space representations. The specificity of the TC methodology is its explicit incorporation of the correlation factor's effects into the Hamiltonian via a similarity transformation [1](#) and [2](#). This yields a non-Hermitian TC Hamiltonian, which although forbids the use of the variational principle for wave function optimization, grants the capacity to make the wave function's expression more compact, and accelerates the convergence toward the complete basis set limit. Furthermore, the effective interaction within the TC Hamiltonian is limited to three-body terms at most, which facilitates the deterministic calculation of all integrals necessary for the optimization of the wave function. This characteristic eliminates the requirement for stochastic sampling of the N -body integrals, a process typically seen in Variational Monte Carlo (VMC) methods.

There are two distinct but connected aspects involved

in the optimization of the wave function within the TC framework: i) the optimization of the correlation factor used to perform the similarity transformation and ii) the optimization of the Slater-determinant part of the wave function.

The role of the correlation factor is quite simple to understand: it fundamentally involves decreasing the probability of finding two electrons at small inter-electronic distances. However, there exists a wide variety of functional forms for the correlation factor which can be broadly divided into two categories: universal two-body correlation factors and three-body correlation factors. Universal correlation factors dependent solely on inter-electronic coordinates and create an homogeneous and isotropic correlation hole throughout the whole space. In contrast, three-body correlation factors present a richer parametrisation, enabling for instance the adaptation of the correlation hole's depth and extension based on the distance of an electron pair from a specific nucleus.

The frozen Gaussian geminal (FROGG), proposed by Ten-No [3](#), was optimized for valence electron pairs and can be seen as the prototype for the universal correlation factor. An alternative universal correlation factor was derived from the range-separated density functional theory [4](#), which depends on a single parameter μ that tailors the shape of the correlation hole. The utilization of a universal correlation factor is appealing due to its minimal optimization requirements. However, it is crucial to note that when enforcing a correlation hole designed for valence electrons in high-density regions,

^{a)}Electronic mail: aammar@irsamc.ups-tlse.fr

^{b)}Electronic mail: emmanuel.giner@lct.jussieu.fr

there is a significant demand for flexibility in the wave function, enough to adapt the density in the core regions. Conversely, three-body correlation factors (for instance, see Refs. 5–15 and references therein) employ explicit electron-electron-nucleus coordinates, allowing for the adjustment of the correlation hole’s depth and spatial extension according to the system’s density, albeit at the expense of extensive optimization. Recently, we introduced a minimal three-body correlation factor¹⁶ which necessitates limited optimization. The performance of this correlation factor will be investigated here.

When it comes to optimizing the Slater-determinant part of the TC wave function, it is important to note that the TC Hamiltonian, as any N -body operator, can be expressed in second quantization. The latter implies that any conventional wave function ansatz from quantum chemistry can be adapted to fit within the TC framework. However, the bi-orthonormal nature of the left and right eigenvectors in the TC Hamiltonian suggests potential change of strategy to choose the basis. Specifically, the latter could be a pair of bi-orthonormal one-electron basis sets to expand both the left and right eigenvectors. This is in contrast to the standard practice of using a single orthonormal one-electron basis set.

Furthermore, replacing a single set of orbitals with two distinct and optimizable sets increases the flexibility of both left and right eigenvectors. This change leads to a decrease in the error associated with the TC energy, which is directly related to the product of the errors in the left and right eigenvectors. Constraining these two sets to form a couple of bi-orthonormal basis helps in defining creation and annihilation operators. These operators fulfill the anti-commutation rules of standard fermionic operators in second-quantized formulations, simplifying the process of adapting any conventional wave function method to the TC framework.

Another important aspect of the TC framework is that the variational principle does not hold anymore due to the non hermitian nature of the TC Hamiltonian. One can nevertheless substitute the energy minimization by the so-called bi variational functional¹. The latter involves finding stationary points of an energy functional depending on both a left and right function. As an example, the optimization of the energy with respect to orbital parameters at the single determinant level necessary leads to two sets of bi orthonormal orbitals adapted for either the left or right eigenvectors.

Taking these peculiar aspects into consideration, we distinguish here between formalisms that use left and right orbitals (termed *bi-orthogonal* frameworks) and those that employ a common set of orbitals (denoted as *orthogonal* formalisms).

Historically, an orthogonal framework utilizing a single Slater determinant was often employed^{1,5,17–31}. Fimple and Unwin’s pioneering work³² introduced a Configura-

tion Interaction (CI) expansion within a bi-orthogonal framework, illustrated on the simple case of the ground state of the Helium atom. Subsequently, the bi-orthogonal formalism was significantly expanded by Ten-*No et al* with Møller-Plesset Perturbation Theory at second order (MP2) and Linearized Coupled Cluster Singles and Doubles (LCCSD) using the FROGG correlation factor in the early 2000s^{3,33–35}. These advances, coupled with efforts on the three-body terms³⁶, enabled calculations on small organic molecules. Recent developments using an orthogonal framework were proposed by several groups using Full Configuration Interaction Quantum Monte Carlo (FCIQMC)^{37–39}, Coupled Cluster (CC)^{40,41}, Matrix Product State (MPS)^{42–44} or CI⁴⁵. Periodic systems also saw applications using either a single Slater determinant, MP2, CI or CC within the orthogonal framework^{46–62}, and later developments using a bi-orthogonal framework were proposed^{63,64}.

In one of our previous work⁶⁵, we introduced Selected CI (SCI) for the TC framework using a single set of orthonormal molecular orbitals within a bi-variational scheme. We observed that enhancing the quality of both the left and right wave functions stabilizes the computation of the second-order perturbative correction. The latter is crucial as it makes the SCI approach competitive by significantly improving the convergence rate of calculations and enabling extrapolation techniques⁶⁶. The quality of the Molecular Orbitals (MOs) is a critical aspect for the practical application of SCI. Specifically, the optimization of orbitals in SCI allows for a more compact CI expansion, either through variationally optimized orbitals^{67–70} or state-average natural orbitals for excited state excitation energies^{71,72}. We would also like to stress the importance of orbital optimization, especially in the context of one of SCI’s primary applications: achieving near CASSCF with a large active space^{67,69,70}. When considering orbital optimization in a bi-variational framework, the bi-orthogonal framework is a natural choice. Hence, the present article aims to further develop SCI within a fully bi-orthonormal and bi-variational framework, i.e. with different left and right molecular orbitals.

In this work, we use a linearized version of the recently developed cheap three-body correlation factor¹⁶. However, we want to highlight that the Bi-Orthogonal (BiO)-SCI proposed here can also be applied with more sophisticated correlation factors, leading to improved convergence properties of the present method.

The structure of the article is the following. Section II A provides a brief overview of the TC framework, then Section II B gives a summary of the bi-variational principle, which is formalized in bi-orthogonal framework in Section II C and then applied to the SCI algorithm in Section II D. We give the explicit form of the correlation factor used here in Section II E. We present the results in Section III, which begins with an investigation of the benefit of using a bi-orthogonal framework for SCI in

Section III B specially regarding the frozen core (fc) approximation which is fundamental in view to apply the TC framework to large systems. Then, we illustrate the convergence of the present BiO-TC-SCI algorithm in Section III C on the F_2 , N_2 and CO molecules, and show that the usual linear extrapolation is possible within our framework. We continue our study by computing the dissociation curve of the CO molecule, which allows us to test the present framework in different regimes of correlation together with the size consistency property. We conclude the present work by computing the atomization energies of a set of 14 molecules in increasing basis sets and compare with both the usual SCI algorithm and estimated exact results. We observe that in most of the case, the accuracy of a calculation in the cc-pVTZ basis set is within 1 kcal/mol with respect to the estimated exact results. We emphasize that no optimization of the correlation factor was needed for molecular systems thanks to the specific form of the correlation factor used here¹⁶. Eventually, we summarize the main results in Section IV.

II. THEORY

A. Basics of the transcorrelated formalism

The general form of the transcorrelated Hamiltonian for a symmetric correlation factor $u(\mathbf{r}_1, \mathbf{r}_2)$ is given by

$$\begin{aligned} \tilde{H}[u] &\equiv e^{-\hat{\tau}_u} \hat{H} e^{\hat{\tau}_u} \\ &= \hat{H} + [\hat{H}, \hat{\tau}_u] + \frac{1}{2} \left[[\hat{H}, \hat{\tau}_u], \hat{\tau}_u \right], \end{aligned} \quad (1)$$

where $\hat{\tau}_u = \sum_{i < j} u(\mathbf{r}_i, \mathbf{r}_j)$ and $\hat{H} = \sum_i -\frac{1}{2} \nabla_i^2 + v(\mathbf{r}_i) + \sum_{i < j} 1/r_{ij}$. Eq. (1) leads to the following transcorrelated Hamiltonian

$$\tilde{H}[u] = \hat{H} - \sum_{i < j} \hat{K}[u](\mathbf{r}_i, \mathbf{r}_j) - \sum_{i < j < k} \hat{L}[u](\mathbf{r}_i, \mathbf{r}_j, \mathbf{r}_k), \quad (2)$$

where the effective two- and three-body operators $\hat{K}[u](\mathbf{r}_1, \mathbf{r}_2)$ and $\hat{L}[u](\mathbf{r}_1, \mathbf{r}_2, \mathbf{r}_3)$ are defined as

$$\begin{aligned} \hat{K}[u](\mathbf{r}_1, \mathbf{r}_2) &= \frac{1}{2} \left(\Delta_1 u(\mathbf{r}_1, \mathbf{r}_2) + \Delta_2 u(\mathbf{r}_1, \mathbf{r}_2) \right. \\ &\quad \left. + (\nabla_1 u(\mathbf{r}_1, \mathbf{r}_2))^2 + (\nabla_2 u(\mathbf{r}_1, \mathbf{r}_2))^2 \right) \\ &\quad + \nabla_1 u(\mathbf{r}_1, \mathbf{r}_2) \cdot \nabla_1 + \nabla_2 u(\mathbf{r}_1, \mathbf{r}_2) \cdot \nabla_2, \end{aligned} \quad (3)$$

and

$$\begin{aligned} \hat{L}[u](\mathbf{r}_1, \mathbf{r}_2, \mathbf{r}_3) &= \nabla_1 u(\mathbf{r}_1, \mathbf{r}_2) \cdot \nabla_1 u(\mathbf{r}_1, \mathbf{r}_3) \\ &\quad + \nabla_2 u(\mathbf{r}_2, \mathbf{r}_1) \cdot \nabla_2 u(\mathbf{r}_2, \mathbf{r}_3) \\ &\quad + \nabla_3 u(\mathbf{r}_3, \mathbf{r}_1) \cdot \nabla_3 u(\mathbf{r}_3, \mathbf{r}_2). \end{aligned} \quad (4)$$

As apparent from the definition of Eq.(1), $\tilde{H}[u]$ is not Hermitian as

$$\tilde{H}^\dagger[u] = e^{+\hat{\tau}_u} \hat{H} e^{-\hat{\tau}_u} \neq \tilde{H}[u], \quad (5)$$

and a given eigenvalue \tilde{E}_i is associated with a couple of right and left eigenvectors

$$\begin{aligned} \tilde{H}[u]|\Phi_i[u]\rangle &= \tilde{E}_i|\Phi_i[u]\rangle \\ \tilde{H}^\dagger[u]|X_i[u]\rangle &= \tilde{E}_i|X_i[u]\rangle. \end{aligned} \quad (6)$$

Nevertheless, thanks to the property of similarity transformations, the spectrum of $\tilde{H}[u]$ coincides with that of the usual Hamiltonian. From thereon, we no longer include the explicit dependence on the correlation factor u , and instead, we will use \tilde{H} , $|X_i\rangle$, and $|\Phi_i\rangle$ to represent the TC Hamiltonian and its corresponding left and right eigenvectors.

B. Non-Hermitian eigenvalue problems and the bi-variational principle

Due to the non-Hermitian nature of the TC Hamiltonian, the standard energy minimization approach cannot be used to optimize wavefunctions since the variational principle does not apply. Instead, the search for an energy minimum over a wavefunction Ψ can be replaced by the search for a stationary point of a functional $\tilde{E}[X, \Phi]$ that depends on two wavefunctions X and Φ

$$\tilde{E}[X, \Phi] = \frac{\langle X | \tilde{H} | \Phi \rangle}{\langle X | \Phi \rangle}, \quad (7)$$

and X and Φ are often referred to as the left and right wavefunctions, respectively. An eigenvalue \tilde{E}_i is obtained when either the left or right function is an eigenfunction.

$$\begin{aligned} \tilde{E}[X, \Phi_i] &= \frac{\langle X | \tilde{H} | \Phi_i \rangle}{\langle X | \Phi_i \rangle} = \tilde{E}_i \forall X, \\ \tilde{E}[X_i, \Phi] &= \frac{\langle X_i | \tilde{H} | \Phi \rangle}{\langle X_i | \Phi \rangle} = \tilde{E}_i \forall \Phi. \end{aligned} \quad (8)$$

Hence, finding \tilde{E}_i and the corresponding left and right eigenvectors is equivalent to nullifying the right and left functional derivatives

$$\begin{aligned} \frac{\delta \tilde{E}[X, \Phi_i]}{\delta X} &= 0 \forall X, \\ \frac{\delta \tilde{E}[X_i, \Phi]}{\delta \Phi} &= 0 \forall \Phi, \end{aligned} \quad (9)$$

which have general forms given by

$$\frac{\delta \tilde{E}[X, \Phi]}{\delta X} = \frac{(\tilde{H}\Phi) \langle X | \Phi \rangle - \langle X | \tilde{H} | \Phi \rangle \Phi}{|\langle X | \Phi \rangle|^2}, \quad (10)$$

$$\frac{\delta \tilde{E}[X, \Phi]}{\delta \Phi} = \frac{(\tilde{H}^\dagger X) \langle X | \Phi \rangle - \langle X | \tilde{H} | \Phi \rangle X}{|\langle X | \Phi \rangle|^2}. \quad (11)$$

This is the so-called bi-variational principle¹. It is worth highlighting that setting the *left* functional derivative to zero for *all left wavefunctions* X enables the determination of the *optimal right wavefunction* (and *vice versa*).

C. Transcorrelation in a bi-orthonormal framework

In this section we briefly summarize how the TC Hamiltonian is written in a bi-orthonormal basis (see Sec. II C 1) and also recall the mathematical framework together with the self-consistent field equations used to obtain the bi-orthonormal basis (see Sec. II C 2).

1. Bi-orthonormal framework and second quantization

In practice, the TC Hamiltonian is projected into a one-particle basis set \mathcal{B}

$$\tilde{H}^{\mathcal{B}} = \hat{P}^{\mathcal{B}} \tilde{H} \hat{P}^{\mathcal{B}}, \quad (12)$$

where $\hat{P}^{\mathcal{B}}$ is the projector onto the Hilbert space spanned by the one-particle basis set \mathcal{B} . Because of the properties of the similarity transformation the exact eigenvalue E_i is recovered in the Complete Basis Set (CBS) limit

$$\lim_{\mathcal{B} \rightarrow \text{CBS}} \tilde{E}_i^{\mathcal{B}} = E_i, \quad (13)$$

and given that some of the correlation effects are accounted for by the correlation factor, we can anticipate a faster convergence of $\tilde{E}_i^{\mathcal{B}}$ compared to wave function methods based on the standard Hamiltonian. For the sake of simplicity in notation, we will henceforth drop the exponent \mathcal{B} and refer directly to $\tilde{H}^{\mathcal{B}}$ as \tilde{H} .

In a second quantization framework, rather than using a standard basis set consisting of real-valued orthonormal spatial MOs $\phi_i(\mathbf{r})$ to express the \tilde{H} operator, a more flexible approach involves using distinct MOs for the left and right functions. The left wave functions are expanded on the set of *left* real-valued orbitals $\mathcal{B}^l = \{\chi_i(\mathbf{r}), i = 1, \dots, n\}$ while the right wave functions are expanded on the set of *right* real-valued orbitals $\mathcal{B}^r = \{\phi_i(\mathbf{r}), i = 1, \dots, n\}$. Similar to the usual orthonormal framework, if the two bases \mathcal{B}^l and \mathcal{B}^r are chosen to satisfy the biorthonormal relation $\langle \chi_i | \phi_j \rangle = \delta_{ij}$, one can build creation operators $\hat{c}_{k,\sigma}^\dagger$ and annihilation operators $\hat{b}_{l,\lambda}$ (where k and l are labels of spin-free orbitals, and σ and λ are labels of spins) that satisfy the usual anticom-

mutation relations^{32,33,73-77}

$$\begin{aligned} [\hat{c}_{k,\sigma}^\dagger, \hat{c}_{l,\lambda}^\dagger]_+ &= 0, \\ [\hat{b}_{k,\sigma}, \hat{b}_{l,\lambda}]_+ &= 0, \\ [\hat{c}_{k,\sigma}^\dagger, \hat{b}_{l,\lambda}]_+ &= \delta_{kl} \delta_{\sigma\lambda}, \end{aligned} \quad (14)$$

and avoid the complications introduced by overlap integrals inherent to the use of non-orthonormal basis functions⁷⁸⁻⁸¹. As a result, expressing an operator in second quantization using the biorthonormal bases \mathcal{B}^l and \mathcal{B}^r involves two straightforward rules: (i) replace the conventional creation and annihilation operators $\hat{a}_{k,\sigma}^\dagger$ and $\hat{a}_{k,\sigma}$ with the biorthonormal basis creation and annihilation operators $\hat{c}_{k,\sigma}^\dagger$ and $\hat{b}_{k,\sigma}$, and (ii) write the integrals of the operator using the functions χ_i in the bra and ϕ_j in the ket.

Following these rules the \tilde{H} operator can be written in a second-quantized form on the two bi-orthonormal basis sets as follows

$$\begin{aligned} \tilde{H} &= \sum_{k \in \mathcal{B}^l} \sum_{i \in \mathcal{B}^r} \sum_{\sigma \in \{\uparrow, \downarrow\}} h_{ki} \hat{c}_{k,\sigma}^\dagger \hat{b}_{i,\sigma} \\ &+ \frac{1}{2} \sum_{k,l \in \mathcal{B}^l} \sum_{i,j \in \mathcal{B}^r} \sum_{\sigma,\lambda \in \{\uparrow, \downarrow\}} (V_{ij}^{kl} - K_{ij}^{kl}) \hat{c}_{k,\sigma}^\dagger \hat{c}_{l,\lambda}^\dagger \hat{b}_{j,\lambda} \hat{b}_{i,\sigma} \\ &- \frac{1}{6} \sum_{k,l,n \in \mathcal{B}^l} \sum_{i,j,m \in \mathcal{B}^r} \sum_{\sigma,\lambda,\kappa \in \{\uparrow, \downarrow\}} L_{ijm}^{kln} \hat{c}_{k,\sigma}^\dagger \hat{c}_{l,\lambda}^\dagger \hat{c}_{n,\kappa}^\dagger \hat{b}_{m,\kappa} \hat{b}_{j,\lambda} \hat{b}_{i,\sigma}, \end{aligned} \quad (15)$$

where h_{ki} and V_{ij}^{kl} are the integrals of the usual one- and two-electron operators, respectively, expressed in the bi-orthonormal basis,

$$h_{ki} = \int d\mathbf{r} \chi_k(\mathbf{r}) \hat{h} \phi_i(\mathbf{r}), \quad (16)$$

$$V_{ij}^{kl} = \int d\mathbf{r}_1 d\mathbf{r}_2 \chi_k(\mathbf{r}_1) \chi_l(\mathbf{r}_2) \frac{1}{r_{12}} \phi_i(\mathbf{r}_1) \phi_j(\mathbf{r}_2), \quad (17)$$

and K_{ij}^{kl} and L_{ijm}^{kln} are the two- and three-electron integrals corresponding to the effective two- and three-body operators $\hat{K}[u](\mathbf{r}_1, \mathbf{r}_2)$ and $\hat{L}[u](\mathbf{r}_1, \mathbf{r}_2, \mathbf{r}_3)$ expressed in the bi-orthonormal basis

$$K_{ij}^{kl} = \int d\mathbf{r}_1 d\mathbf{r}_2 \chi_k(\mathbf{r}_1) \chi_l(\mathbf{r}_2) \hat{K}[u](\mathbf{r}_1, \mathbf{r}_2) \phi_i(\mathbf{r}_1) \phi_j(\mathbf{r}_2), \quad (18)$$

$$L_{ijm}^{kln} = \int d\mathbf{r}_1 d\mathbf{r}_2 d\mathbf{r}_3 \chi_k(\mathbf{r}_1) \chi_l(\mathbf{r}_2) \chi_n(\mathbf{r}_3) \hat{L}[u](\mathbf{r}_1, \mathbf{r}_2, \mathbf{r}_3) \phi_i(\mathbf{r}_1) \phi_j(\mathbf{r}_2) \phi_m(\mathbf{r}_3). \quad (19)$$

An important consequence of the bi-orthonormal framework is the one-to-one correspondence between the left and right Slater determinants even if they are built with different functions. To illustrate this, let us consider a left Slater determinant $\langle X_I | = \prod_{i \in S_{X_I}}^N \langle 0 | \hat{b}_i$ where

$\mathcal{S}_{X_I} = \{k\}$ is the ordered list of indices of left orbitals $\chi_k(\mathbf{r})$ occupied in $\langle X_I |$. In a similar way, let us consider a right Slater determinant $|\Phi_J\rangle = \prod_{i \in \mathcal{S}_{\Phi_J}} \hat{c}_i^\dagger |0\rangle$ where $\mathcal{S}_{\Phi_J} = \{l\}$ is the ordered list of indices of right orbitals $\phi_l(\mathbf{r})$ occupied in $|\Phi_J\rangle$. Because of the bi-orthonormality relation, these two Slater determinants are orthogonal only if the two sets \mathcal{S}_{X_I} and \mathcal{S}_{Φ_J} are different

$$\begin{aligned} \langle X_I | \Phi_J \rangle &= 0 \quad \text{if } \mathcal{S}_{X_I} \neq \mathcal{S}_{\Phi_J}, \\ &= 1 \quad \text{if } \mathcal{S}_{X_I} = \mathcal{S}_{\Phi_J}. \end{aligned} \quad (20)$$

As a consequence, to each right Slater determinant $|\Phi_J\rangle$ one can associate a unique left Slater determinant $\langle X_I |$ with an identical list of indices of occupied orbitals, although the orbitals composing these two Slater determinants are themselves different.

2. Optimization of bi-orthonormal orbitals in the TC framework

The selection of orbitals used to expand the wave function is a crucial factor in enhancing the accuracy of any approximated wave function ansatz. In the Hermitian case, the starting point is often the set of Hartree-Fock (HF) orbitals, as they minimize the energy of a single Slater determinant wave function. However, in the case of the TC Hamiltonian, which is a non-Hermitian operator, the expectation value of a single Slater determinant cannot be minimized. Instead, one can seek a stationary point of the functional $\tilde{E}[X, \Phi]$, where both X and Φ are single-determinant wave functions. It's important to note that these wave functions are not necessarily built with the same orbitals. Using reference determinants X_0 and Φ_0 constructed on two bi-orthonormal basis sets, \mathcal{B}^l and \mathcal{B}^r respectively, and with the same orbital occupancy, we can write the left and right single Slater determinant wave function as follows

$$\begin{aligned} |\Phi[\hat{\kappa}]\rangle &= e^{\hat{\kappa}} |\Phi_0\rangle, \\ \langle X[\hat{\kappa}] | &= e^{\hat{\kappa}} \langle X_0 |. \end{aligned} \quad (21)$$

Here $\hat{\kappa}$ are anti hermitian orbital rotation operators

$$\hat{\kappa} = \sum_{p>q} \kappa_{pq} \hat{E}_{pq}, \quad (22)$$

with the operators \hat{E}_{pq} being defined as

$$\hat{E}_{pq} = \sum_{\sigma \in \{\uparrow, \downarrow\}} \hat{c}_{p,\sigma}^\dagger \hat{b}_{q,\sigma}, \quad (23)$$

and where the κ_{pq} are the orbital rotation parameters forming the matrix $\boldsymbol{\kappa}$. The fact that we use a single set of orbital parameters $\boldsymbol{\kappa}$ even if we optimize two distinct functions is due to the bi-orthonormal condition which ensures

$$\begin{aligned} \langle X[\hat{\kappa}] | \Phi[\hat{\kappa}] \rangle &= \langle X_0 | e^{-\hat{\kappa}} e^{\hat{\kappa}} | \Phi_0 \rangle \\ &= \langle X_0 | \Phi_0 \rangle = 1. \end{aligned} \quad (24)$$

In other words, the bi-orthonormal condition imposes that the left orbitals are related to the right orbitals through the matrix \mathbf{S}^{-1} , where \mathbf{S} is the overlap matrix between the right orbitals. Another point is that the matrix of the orbital parameters $\boldsymbol{\kappa}$ is no longer anti hermitian but fulfills a pseudo anti hermitian relation

$$(\boldsymbol{\kappa})^\dagger = -\mathbf{S}\boldsymbol{\kappa}\mathbf{S}^{-1}. \quad (25)$$

The equivalent of the standard energy minimization condition in the HF framework translates within the TC context in seeking a stationary point of the following functional:

$$\tilde{E}[\hat{\kappa}] = \frac{\langle X_0 | e^{-\hat{\kappa}} \tilde{H} e^{\hat{\kappa}} | \Phi_0 \rangle}{\langle X_0 | e^{-\hat{\kappa}} e^{\hat{\kappa}} | \Phi_0 \rangle}. \quad (26)$$

and, using Eq. (24), the functional $\tilde{E}[\hat{\kappa}]$ can be written up to first-order in $\hat{\kappa}$ as

$$\tilde{E}[\hat{\kappa}] = \langle X_0 | \tilde{H} | \Phi_0 \rangle - \langle X_0 | \hat{\kappa} \tilde{H} | \Phi_0 \rangle + \langle X_0 | \tilde{H} \hat{\kappa} | \Phi_0 \rangle + o(|\hat{\kappa}|^2). \quad (27)$$

Differentiating Eq. (27) with respect to κ_{pq} and evaluating at $\boldsymbol{\kappa} = 0$ leads to

$$\left. \frac{\partial \tilde{E}[\hat{\kappa}]}{\partial \kappa_{pq}} \right|_{\boldsymbol{\kappa}=0} = \langle X_0 | \tilde{H} \hat{E}_{pq} | \Phi_0 \rangle - \langle X_0 | \hat{E}_{pq} \tilde{H} | \Phi_0 \rangle. \quad (28)$$

We assume here closed shell determinants and label the occupied and virtual orbitals by i and a , respectively. By noticing that $\langle X_0 | \hat{E}_{ai} = 0 = \hat{E}_{ia} | \Phi_0 \rangle$, canceling the derivative with respect to occupied-virtual orbital rotation parameters leads to

$$\left. \frac{\partial \tilde{E}[\hat{\kappa}]}{\partial \kappa_{ia}} \right|_{\boldsymbol{\kappa}=0} = 0 \Leftrightarrow \langle X_0 | \hat{E}_{ia} \tilde{H} | \Phi_0 \rangle = 0, \quad (29)$$

and

$$\left. \frac{\partial \tilde{E}[\hat{\kappa}]}{\partial \kappa_{ai}} \right|_{\boldsymbol{\kappa}=0} = 0 \Leftrightarrow \langle X_0 | \tilde{H} \hat{E}_{ai} | \Phi_0 \rangle = 0, \quad (30)$$

which give the left and right Brillouin conditions for the set of orbitals composing $|X_0\rangle$ and $|\Phi_0\rangle$. Of course, all this derivation is trivially extendable to the open shell case.

Just like in the Hermitian case, these Brillouin conditions can be fulfilled by iteratively diagonalizing a Fock-like operator. Within the TC framework, the corresponding Fock operator is non-Hermitian and constructed not with a standard density, but with a transition density between the left and right functions. Using matrix notations, the transition density \mathbf{D} can be written in the Atomic Orbital (AO) basis as

$$\mathbf{D} = \mathbf{C}_L^\dagger \mathbf{C}_R, \quad (31)$$

where \mathbf{C}_L (\mathbf{C}_R) represents the matrix of coefficients of occupied left (right) orbitals on the AO basis. The interested reader can look for instance in Ref. 16 where an explicit form of the Fock operator is given.

D. Development of selected CI in a bi-orthonormal framework

In this section we describe the theoretical background of the TC-SCI in the bi-orthonormal framework. This requires first the development of a Rayleigh-Schrödinger perturbation theory using the bi-variational principle as the starting point and adapting it to a bi-orthonormal basis (Sec. IID 1). We then give the explicit algorithm used for our BiO-TC-SCI algorithm in Sec. IID 2, together with the technical details in Sec. IID 3.

1. Perturbation theory of the functional

Following Ref. 65 we give the perturbation expansion of the functional $\tilde{E}[X, \Phi]$ for the ground-state energy. Here, the derivation is adapted to the bi-orthonormal framework.

Let the Hamiltonian \tilde{H} be split into

$$\tilde{H} = \tilde{H}_0 + \lambda \tilde{V}. \quad (32)$$

We assume that the left and right eigenvectors of \tilde{H}_0 are known,

$$\begin{aligned} \tilde{H}_0 |\Phi_i\rangle &= \epsilon_i |\Phi_i\rangle \\ \tilde{H}_0^\dagger |X_i\rangle &= \epsilon_i |X_i\rangle, \end{aligned} \quad (33)$$

and that they form a bi-orthonormal set

$$\langle X_i | \Phi_j \rangle = \delta_{ij}. \quad (34)$$

In the case of a SCI theory within an Epstein Nesbet (EN)^{82,83} partitioning, $|X_0\rangle$ and $|\Phi_0\rangle$ are the ground state left and right eigenvectors of \tilde{H}_0 (which can be multi configurational) while the $|X_i\rangle$ and $|\Phi_i\rangle$ for $i > 0$ are Slater determinants such that $\langle X_0 | \Phi_i \rangle = \langle X_i | \Phi_0 \rangle = 0$. The ground-state energy \tilde{E}_{gs} can be obtained by evaluating $\tilde{E}[X, \Phi_{\text{gs}}]$, *i.e.* evaluating the functional at the right ground-state wave function, but the choice of X remains. Based on our previous numerical study⁶⁵, we choose $|X\rangle = |X_0\rangle$, *i.e.* the left eigenfunction of \tilde{H}_0 . The functional then reads

$$\tilde{E}[X_0, \Phi_{\text{gs}}] = \frac{\langle X_0 | \tilde{H}_0 + \lambda \tilde{V} | \Phi_{\text{gs}} \rangle}{\langle X_0 | \Phi_{\text{gs}} \rangle}. \quad (35)$$

We now expand the ground-state energy in powers of λ

$$\tilde{E}[X_0, \Phi_{\text{gs}}] = \sum_{k=0}^{\infty} \lambda^k \tilde{E}^{(k)}, \quad (36)$$

which therefore implies to also expand the right eigenvector in powers of λ

$$|\Phi_{\text{gs}}\rangle = \sum_{k=0}^{\infty} \lambda^k |\Phi^{(k)}\rangle, \quad (37)$$

where $|\Phi^{(k)}\rangle$ is the correction to the right ground state wave function at the order k which is expanded in the basis of the right eigenvectors of \tilde{H}_0 assuming intermediate bi-orthonormalization

$$|\Phi^{(k)}\rangle = \sum_i c_i^{(k)} |\Phi_i\rangle, \quad (38)$$

$$\langle X_0 | \Phi^{(k)} \rangle = 0 \quad \text{if } k \neq 0,$$

which implies, because of the bi-orthonormality property, that $\langle X_0 | \Phi_{\text{gs}} \rangle = 1$.

Truncating up to second order Eq. (36) leads to

$$\tilde{E}[X_0, \Phi_{\text{gs}}] = \tilde{E}^{(0)} + \lambda \tilde{E}^{(1)} + \lambda^2 \tilde{E}^{(2)}, \quad (39)$$

which then yields

$$\begin{aligned} \tilde{E}^{(0)} &= \langle X_0 | \tilde{H}_0 | \Phi^{(0)} \rangle, \\ \tilde{E}^{(1)} &= \langle X_0 | \tilde{V} | \Phi^{(0)} \rangle, \\ \tilde{E}^{(2)} &= \langle X_0 | \tilde{V} | \Phi^{(1)} \rangle. \end{aligned} \quad (40)$$

To obtain the equation for the perturbed wave function one replaces the expressions of both $|\Phi_{\text{gs}}\rangle$ and $\tilde{E}[X_0, \Phi_{\text{gs}}]$ in Eq. (35) and for $\Phi^{(1)}$, which then leads to

$$\tilde{H}_0 |\Phi^{(1)}\rangle + \tilde{V} |\Phi^{(0)}\rangle = \tilde{E}^{(0)} |\Phi^{(1)}\rangle + \tilde{E}^{(1)} |\Phi^{(0)}\rangle. \quad (41)$$

By projecting Eq. (41) on a function $|X_i\rangle$ one obtains the expression of the coefficient of the right function at first order

$$c_i^{(1)} = \frac{\langle X_i | \tilde{V} | \Phi^{(0)} \rangle}{\tilde{E}^{(0)} - \epsilon_i}, \quad (42)$$

and therefore one can obtain the second order contribution to the energy

$$\tilde{E}^{(2)} = \sum_{i=1}^N \tilde{E}_i^{(2)}, \quad (43)$$

where $\tilde{E}_i^{(2)}$ is the contribution at second order to the energy of the function $|\Phi_i\rangle$

$$\begin{aligned} \tilde{E}_i^{(2)} &= \langle X_0 | \tilde{V} | \Phi_i \rangle c_i^{(1)} \\ &= \frac{\langle X_0 | \tilde{V} | \Phi_i \rangle \langle X_i | \tilde{V} | \Phi^{(0)} \rangle}{\tilde{E}^{(0)} - \epsilon_i}. \end{aligned} \quad (44)$$

With respect to the standard Hermitian case, one can notice here several differences in Eqs. (42) and (44): i) The first-order coefficient $c_i^{(1)}$ is computed using $\langle X_i | \tilde{V} | \Phi^{(0)} \rangle$, implying therefore the use of the left function X_i satisfying $\langle X_i | \Phi_i \rangle = 1$. This is a consequence of the bi-orthonormal framework, as in the case of an orthonormal framework, the function X_i would be simply equal to Φ_i . ii) The computation of the energy implies in the general case, through $\langle X | \tilde{V} | \Phi_i \rangle$, the use of a left function X , that we chose here to be $|X_0\rangle$.

One could also expand in perturbation the left eigenvector $|X_{\text{gs}}\rangle$, and evaluate the functional at the right function $|\Phi_0\rangle$. In that case, one would obtain exactly the same expansion for the energy up to second-order.

2. Selected CI algorithm in a bi-orthonormal framework

In Ref. 65 we investigated the various flavours of TC-SCI using an orthonormal framework. Among the different choices of selection criteria tested, we found that the one based on the second-order contribution to the energy using both the left and right eigenvectors of \tilde{H}_0 as zeroth order wave function was the most efficient because it allows to improve both the left and right eigenvectors. We therefore follow a similar path here, using an EN zeroth-order Hamiltonian, and present our bi-orthonormal TC-SCI (BiO-TC-SCI) algorithm which, at an iteration n , can be summarized as follows.

1. A given zeroth order set of right Slater determinants $\mathcal{P}_r^n = \{|\Phi_I\rangle, I = 1, \dots, N_{\text{det}}\}$ is known, and therefore its associated left zeroth order set is also known $\mathcal{P}_l^n = \{|X_I\rangle, I = 1, \dots, N_{\text{det}}\}$. One obtains then the ground state left and right eigenvectors of the TC-Hamiltonian within \mathcal{P}_l^n and \mathcal{P}_r^n

$$\begin{aligned}\tilde{H}^\dagger |X^{(0)}\rangle &= \tilde{E}^{(0)} |X^{(0)}\rangle, \\ \tilde{H} |\Phi^{(0)}\rangle &= \tilde{E}^{(0)} |\Phi^{(0)}\rangle,\end{aligned}\quad (45)$$

with

$$\begin{aligned}|X^{(0)}\rangle &= \sum_{I \in \mathcal{P}_l^n} d_I^{(0)} |X_I\rangle, \\ |\Phi^{(0)}\rangle &= \sum_{I \in \mathcal{P}_r^n} c_I^{(0)} |\Phi_I\rangle.\end{aligned}\quad (46)$$

2. For each Slater determinant $|\Phi_I\rangle \notin \mathcal{P}_r^n$, estimate its importance thanks to its contribution to the energy at second-order using the EN zeroth-order Hamiltonian

$$\tilde{E}_I^{(2)} = \frac{\langle X^{(0)} | \tilde{H} | \Phi_I \rangle \langle X_I | \tilde{H} | \Phi^{(0)} \rangle}{\tilde{E}^{(0)} - \epsilon_I}, \quad (47)$$

where $\epsilon_I = \langle X_I | \tilde{H} | \Phi_I \rangle$. We also compute on the fly the total second-order contribution to the energy

$$\tilde{E}^{(2)} = \sum_{I \notin \mathcal{P}_r^n} \tilde{E}_I^{(2)}, \quad (48)$$

and estimate the energy as

$$E_{\text{TC-CIPSI}} = \tilde{E}^{(0)} + \tilde{E}^{(2)}. \quad (49)$$

3. Select the set of N_{Φ_I} right Slater determinants $\{|\Phi_I\rangle\}$, labelled \mathcal{A}_r^n , with the largest $|\tilde{E}_I^{(2)}|$. This automatically defines the corresponding set of left Slater determinants \mathcal{A}_l^n .
4. Add the set \mathcal{A}_r^n to \mathcal{P}_r^n and \mathcal{A}_l^n to \mathcal{P}_l^n to define the new set of both left and right Slater determinants of the zeroth order space

$$\begin{aligned}\mathcal{P}_r^{n+1} &= \mathcal{P}_r^n \cup \mathcal{A}_r^n, \\ \mathcal{P}_l^{n+1} &= \mathcal{P}_l^n \cup \mathcal{A}_l^n.\end{aligned}\quad (50)$$

5. Go back to step 1 and iterate until a given convergence criterion is reached.

3. Technical details about the BiO-TC-SCI algorithm

The computation of TC Hamiltonian matrix elements for the diagonalization step of Eq.(45) is done within the so-called 5-idx approximation introduced in Ref. 39 which consists in neglecting the pure triple excitation terms in the three-body operator, *i.e.* the terms involving integrals L_{ijm}^{klm} with six distinct indices in Eq.(15). In addition, when selecting a given Slater determinant we automatically include all other Slater determinants belonging to the configuration space functions (CSF) in which the determinant is involved, such that pure spin states are obtained after diagonalization. The diagonalization is made using two distinct Davidson procedures: one for the left and one for the right eigenvectors, following Ref. 84.

As the computation of $\tilde{E}^{(2)}$ is costly, we neglect all contributions from the three-electron operator in Eqs. (47) and (49), and also adapt the stochastic version proposed in Ref. 85. In the original algorithm, external determinants are organized in batches generated from a determinant of the internal space. The batch generated by $|I\rangle$ is drawn with a probability $|c_I^{(0)}|^2 / \sum_J |c_J^{(0)}|^2$. In the present work, the batches are drawn with a probability $|d_I^{(0)} c_I^{(0)}| / \sum_J |d_J^{(0)} c_J^{(0)}|$.

Finally, we use the extrapolation technique of Ref. 66 which allows to estimate the TC-Full Configuration Interaction (FCI) energy as the zeroth-order energy $\tilde{E}^{(0)}$ obtained for a vanishing $\tilde{E}^{(2)}$.

E. A simple three-body correlation factor for frozen-core calculations

Although the BiO-TC-SCI algorithm presented here is applicable to any form of correlation factor, we focus on a linearized version of the simple three-body correlation factor developed in Ref. 16. The correlation factor reads

$$\mathcal{U}(\mathbf{r}_1, \mathbf{r}_2, \mu, \{\alpha_i\}) = u(r_{12}, \mu) \bar{g}(\mathbf{r}_1) \bar{g}(\mathbf{r}_2), \quad (51)$$

where $u(r_{12}, \mu)$ is the one-parameter correlation factor introduced in Ref. 4,

$$u(r_{12}, \mu) = \frac{1}{2} r_{12} \left(1 - \text{erf}(\mu r_{12}) \right) - \frac{1}{2\sqrt{\pi}\mu} e^{-(\mu r_{12})^2}, \quad (52)$$

and the envelope

$$\bar{g}(\mathbf{r}) = 1 - \sum_{m=1}^{N_{\text{nuc1}}} \exp(-\alpha_m |\mathbf{r} - \mathbf{R}_m|^2), \quad (53)$$

is the linearized version of the function introduced in Ref. 16, with \mathbf{R}_m the position of the m -th nucleus in the system. The envelope $\bar{g}(\mathbf{r})$ plays the role of a damping function which suppresses the effect of the correlation factor $u(r_{12}, \mu)$ near each nucleus. The parameters α_m control the typical range on which the correlation factor $u(r_{12}, \mu)$ is killed by the envelope $\bar{g}(\mathbf{r}_1)\bar{g}(\mathbf{r}_2)$ around the nucleus located at \mathbf{R}_m . The advantages of this relatively simple correlation factor are that, as shown in Ref. 16, i) an efficient analytical-numerical scheme can be used to obtain the integrals K_{ij}^{kl} and L_{ijm}^{kln} , ii) provided that a typical valence value of the μ parameter is given ($\mu = 0.87$), the correlation factor has only one parameter for each nucleus in the molecule, iii) the parameters α_m are transferable, and can be optimized only for the isolated atoms.

III. RESULTS

A. Computational details

The BiO-TC-SCI code, with all required integrals, has been implemented in the Quantum Package software⁸⁶. The computation of integrals is based on a mixed analytical-numerical integration scheme, as detailed in Ref. 16.

All computations are carried out using the cc-pVXZ Dunning family of basis sets. The TC calculations have been performed with the correlation factor as detailed in Sec. II E. For each atom with a nuclear charge Z_m , the corresponding nuclear parameter α_m is determined as the minimum of a VMC calculation for that atom using a single Slater determinant. This determinant is constructed with orbitals that are the right eigenvalues of the TC-Fock operator in the cc-pVTZ basis set (for more details, see Ref. 16). The only exception is the hydrogen atom, for which we take $\alpha_H = \infty$, as it has no core electrons. We adhere to the strategy of having a unique nuclear parameter α_m for each atom, regardless of the basis set used, and we do not re-optimize these parameters in the molecular systems. This approach results in a correlation factor that does not require any system-specific optimization.

The parameters α_m used in this study are presented in Table I. All the BiO-TC-SCI energies are calculated using the extrapolation scheme described in Sec. II D 3. Unless explicitly stated otherwise, all calculations are performed within the frozen core approximation with a [He] core.

TABLE I. Parameters α_m used in the present work.

Atom	H	Li	C	N	O	F	Ne
α_m	∞	5.5	2.5	2.5	2.0	2.0	2.0

B. Benefits of bi-orthogonal orbital optimization: freezing core orbitals and linear extrapolation

Core electrons have an important property: they contribute minimally to most chemically relevant energy differences, such as Ionization Potentials (IPs) or Atomization Energies (AEs). This property is leveraged in virtually all post-HF methods by using the fc approximation, significantly reducing the computational cost, especially when using strong scaling methods like SCI or CC. However, this technique depends on the optimization of core orbitals such that i) excitations of electrons from these orbitals to valence orbitals have a negligible weight in the wave functions of the low energy part of the spectrum, and ii) the core-core and core-valence correlation energy are essentially transferable from atoms to molecules. The most straightforward way to achieve this decoupling between core and valence orbitals is to obtain eigenvectors of the Fock matrix, i.e., perform a canonical HF optimization.

Transitioning to the context of the TC Hamiltonian, given that the effective interaction is no longer the Coulomb interaction, there is no reason for the usual core electrons HF orbitals to achieve the decoupling necessary for the fc approximation. A logical approach is then to perform the equivalent of the HF orbital optimization adapted for the TC Hamiltonian. This results in a bi-variational and bi-orthogonal framework as described in Sec. II C 2.

To examine the impact of the quality of core orbitals used in TC calculations on typical valence energy differences, we computed the IPs of oxygen, fluorine, and neon atoms, along with the AE of the F_2 molecule. These computations were performed in the cc-pVTZ basis set, with or without the fc approximation, using conventional SCI, or the TC-SCI with either Restricted Hartree-Fock (RHF) orbitals or bi-orthogonal orbitals. The results of these computations are presented in Table II. As can be seen from Table II, the fc approximation affects both the IPs and AE by a few tenths of mH when using the standard SCI. This is typically what is expected for such an energy difference driven by valence properties. In the context of the TC-SCI framework, a variation of the same order of magnitude is observed when using the bi-orthogonal orbitals, while variation by an order of magnitude larger is observed when using the RHF orbitals. More importantly, it can be observed that when using RHF orbitals, the variation on the IPs with the fc approximation increases with the nuclear charge. It is

1 kcal/mol, 1.4 kcal/mol, and 2.0 kcal/mol for the oxygen, fluorine, and neon atoms, respectively. Also, the impact of the fc approximation on the AE of the F_2 molecule is about 1.4 kcal/mol. However, the all-electron TC calculations using both RHF and bi-orthogonal orbitals agree within a few tenths of mH. The small deviation of the AE from the RHF and bi-orthogonal calculations originates from the 5-idx approximation, which does not guarantee strict orbital invariance as part of the Hamiltonian is truncated.

Another notable characteristic of the bi-orthogonal orbitals is that they facilitate a more straightforward linear extrapolation of $\tilde{E}^{(0)}$ as a function of $\tilde{E}^{(2)}$. The latter is crucial for obtaining reliable estimates of the TC-FCI energy. To illustrate this, we present in Fig. 1 the variation of $\tilde{E}^{(0)}$ as a function of $\tilde{E}^{(2)}$ for the all-electron calculation of the F_2 molecule in the cc-pVTZ basis set. As can be seen from Fig. 1, the TC-SCI exhibits more linearity when performed using bi-orthogonal orbitals than when using RHF orbitals. Upon careful examination of the data, it appears that this difference arises from the amount of positive contribution to $\tilde{E}^{(2)}$, which is typically ten times larger when using RHF orbitals, as illustrated in Fig. 1.

These results underscore the importance of optimizing the orbitals within a bi-orthogonal framework when performing TC calculations. This optimization is key for enabling the fc approximation along with extrapolation techniques, which are essential for the application of the method to large systems and/or active spaces.

TABLE II. Ionization potentials (IP) and atomization energy (AE), in mH, computed with TC-SCI in a cc-pVTZ basis set, with (fc) or without (all-e) the frozen core approximation, and using either the usual HF orbitals (RHF) orbitals or the bi-orthogonal TC-SCF orbitals (BiO). Usual hermitian SCI values are also reported.

	SCI	TC-SCI@RHF	TC-SCI@BiO
IP of the oxygen atom			
all-e	489.85	496.04	495.87
fc	489.75	497.74	495.86
IP of the fluorine atom			
all-e	630.00	636.82	636.62
fc	629.80	639.08	636.55
IP of the neon atom			
all-e	783.09	789.85	789.88
fc	782.80	793.02	789.68
AE of the F_2 molecule			
all-e	56.76	61.05	61.69
fc	56.39	63.28	61.47

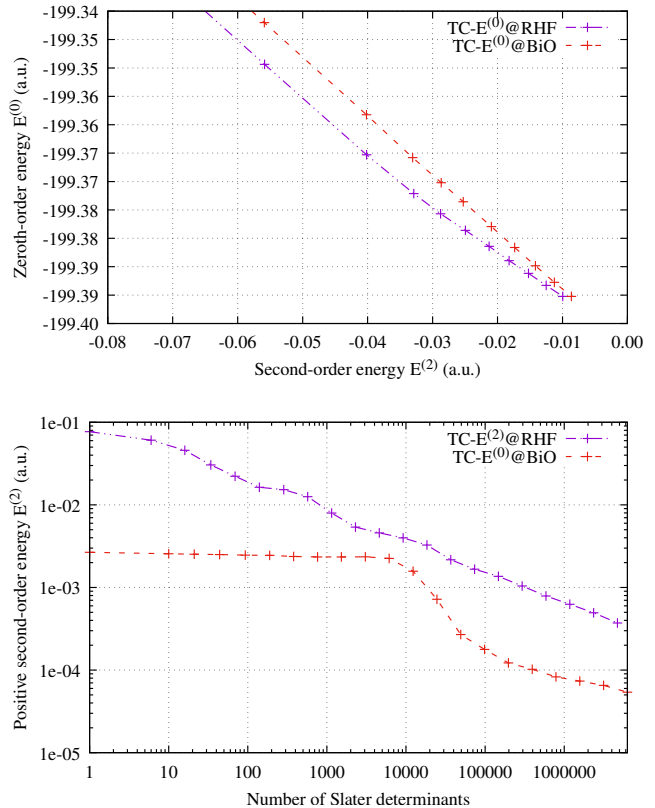


FIG. 1. F_2 , equilibrium geometry, cc-pVTZ basis set: a) Convergence of $\tilde{E}^{(0)}$ using either RHF orbitals (TC- $E^{(0)}$ @RHF) or TC-SCF orbitals (TC- $E^{(0)}$ @BiO) as a function of $\tilde{E}^{(2)}$. b) Convergence of the positive contributions of $\tilde{E}^{(2)}$ using either TC-SCF or RHF orbitals.

C. Convergence of the BiO-TC-SCI algorithm

To illustrate the convergence of the current BiO-TC-SCI algorithm, we present the convergence of $\tilde{E}^{(0)}$, $\tilde{E}^{(2)}$ and $E_{\text{TC-CIPSI}}$ (see Eqs. (45), (48), and (49), respectively) as a function of the number of Slater determinants for the F_2 , N_2 , and CO molecules in the cc-pVTZ basis set (Figs. 2, 3, and 4, respectively). We also include the extrapolation towards the TC-FCI energy, as is typically done in SCI calculations. For comparison, the convergence of the standard SCI scheme is also reported.

From Figs. 2, 3 and 4, it clearly appears that the convergence of the BiO-TC-SCI algorithm is at least as fast as in usual SCI algorithms, and that it can also be effectively extrapolated using a linear fitting. When examining the convergence curve of $\tilde{E}^{(2)}$ as a function of the number of Slater determinants, it is apparent that $|\tilde{E}^{(2)}|$ is consistently smaller than when using the bare Hamiltonian. This is due to the correlation factor already accounting for a portion of the correlation. However, the correlation factor proposed in this study is not re-optimized for each molecular situation, and therefore a signif-

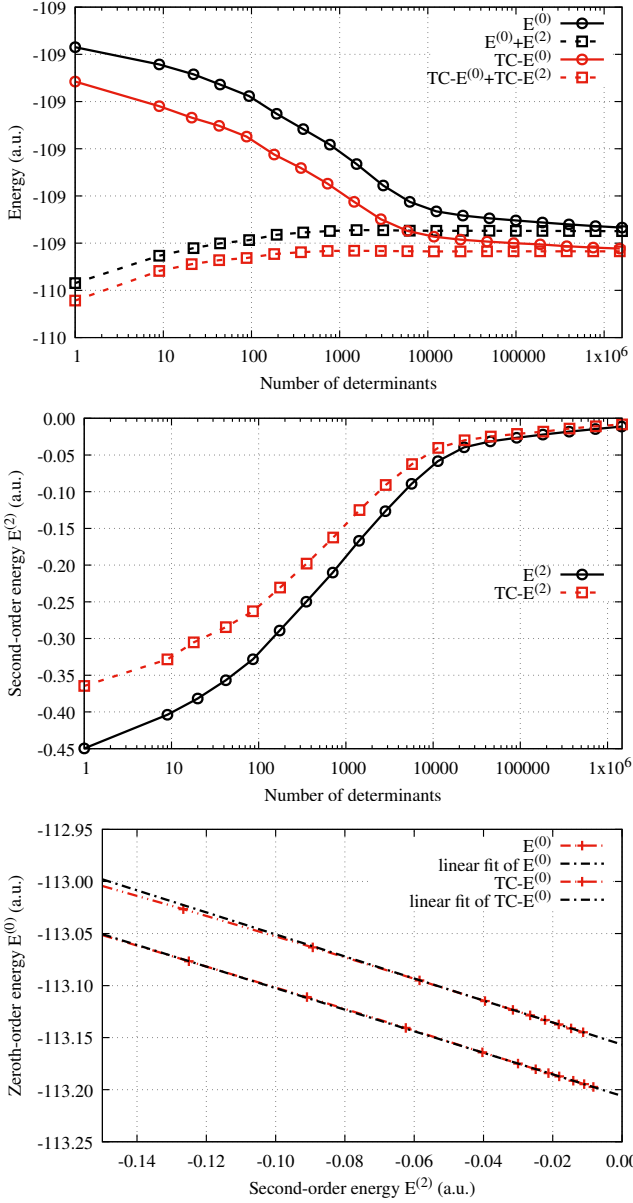


FIG. 2. F_2 , equilibrium geometry, cc-pVTZ basis set: Convergence of $\tilde{E}^{(0)}$ ($TC-E^{(0)}$), $\tilde{E}^{(2)}$ ($TC-E^{(2)}$), and $E_{TC-CIPSI}$ ($TC-E^{(0)}+TC-E^{(2)}$) (see Eqs. (45), (48), and (49), respectively) as a function of the number of Slater determinants. The corresponding usual quantities are also reported for comparison, and are denoted without the “TC” prefix. The convergence of $\tilde{E}^{(0)}$ as a function of $\tilde{E}^{(2)}$ is also reported, together with a linear fit of the data.

icant part of the electron-electron correlation need to be represented by the determinantal component of the wave function. This is why the typical effect of wave function compaction is not significantly evident. Employing more advanced forms of Jastrow factors would further reduce $|\tilde{E}^{(2)}|$, leading to a faster convergence of the SCI energy.

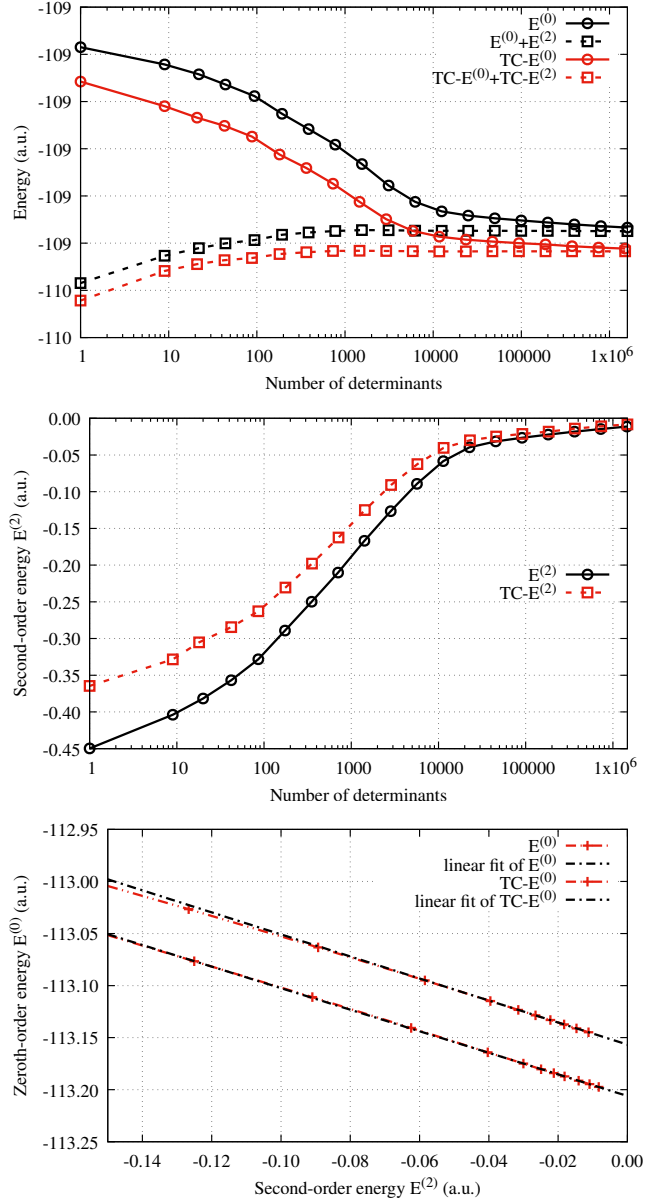


FIG. 3. N_2 , equilibrium geometry, cc-pVTZ basis set: Convergence of $\tilde{E}^{(0)}$ ($TC-E^{(0)}$), $\tilde{E}^{(2)}$ ($TC-E^{(2)}$), and $E_{TC-CIPSI}$ ($TC-E^{(0)}+TC-E^{(2)}$) (see Eqs. (45), (48), and (49), respectively) as a function of the number of Slater determinants. The corresponding usual quantities are also reported for comparison, and are denoted without the “TC” prefix. The convergence of $\tilde{E}^{(0)}$ as a function of $\tilde{E}^{(2)}$ is also reported, together with a linear fit of the data.

D. Ability to break multiple covalent bonds and size consistency

To explore the potential of the current BiO-TC-SCI approach in handling strongly correlated systems, we present in Fig. 5 the potential energy surface (PES) of the CO molecule, using the cc-pVTZ basis set, up to the

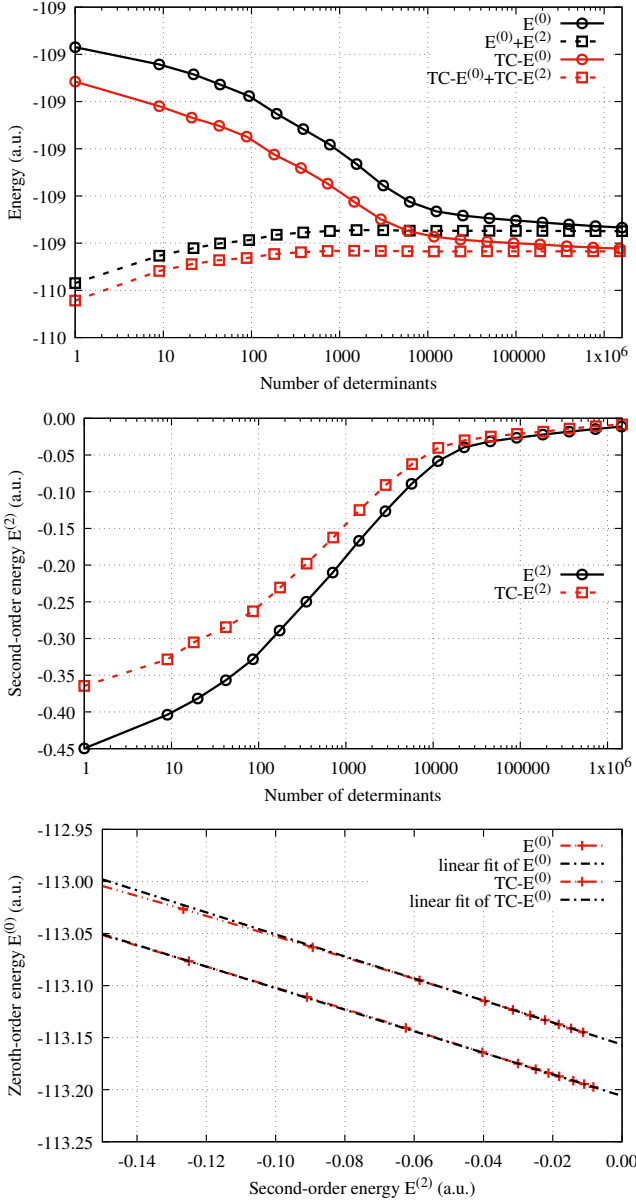


FIG. 4. CO, equilibrium geometry, cc-pVTZ basis set: Convergence of $\tilde{E}^{(0)}$ ($TC-E^{(0)}$), $\tilde{E}^{(2)}$ ($TC-E^{(2)}$), and $E_{TC-CIPSI}$ ($TC-E^{(0)}+TC-E^{(2)}$) (see Eqs. (45), (48), and (49), respectively) as a function of the number of Slater determinants. The corresponding usual quantities are also reported for comparison, and are denoted without the “TC” prefix. The convergence of $\tilde{E}^{(0)}$ as a function of $\tilde{E}^{(2)}$ is also reported, together with a linear fit of the data.

full dissociation limit. This is compared with the sum of the TC energies obtained at the same level of calculation for the isolated atomic systems. As can be seen from Fig. 5, the PES is smooth across the curve and converges towards the correct asymptotic limit, even for a non-homogeneous system. This is because the extrapolated BiO-TC-SCI achieves near TC-FCI quality, and the three-body correlation factor used in this study is

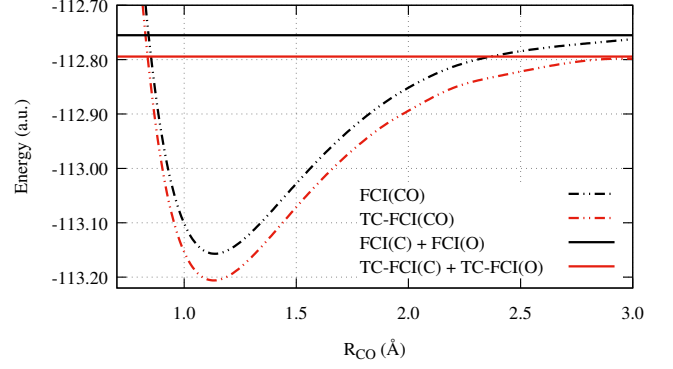


FIG. 5. CO, cc-pVTZ basis set: Potential energy curve computed using the extrapolated energies E_{FCI} and E_{TC-FCI} . The sum of the extrapolated $E_{FCI}(C) + E_{FCI}(O)$ and $E_{TC-FCI}(C) + E_{TC-FCI}(O)$ energies for the isolated atoms are also reported.

size consistent.

Additionally, we incorporate the PES obtained through the standard extrapolated FCI into the same figure. A comparison between the two PESs reveals a more pronounced and deeper well in the curve for the BiO-TC-SCI approach. This result further substantiates the enhanced ability of BiO-TC-SCI to effectively manage the electron correlation effects within the system.

E. Atomization energies

Table III presents the atomization energy results (in mH) for a selection of molecules using the standard extrapolated FCI or the extrapolated TC-FCI. These calculations were performed in various basis sets, specifically cc-pVDZ, cc-pVTZ, and cc-pVQZ for the FCI, and cc-pVDZ and cc-pVTZ for the TC-FCI. In addition to the calculated results, the “estimated exact” column provides an estimation of the exact non-relativistic atomization energies, sourced from Ref. 87. This serves as a benchmark for the accuracy of the methods used. The molecular geometries were also taken from Ref. 87. To supplement the data in the table, we provide a visual representation of the FCI (E_{FCI}) and TC-FCI (E_{TC-FCI}) results in the cc-pVQZ and cc-pVTZ basis sets, respectively, in Figure 6. This aids in interpreting and demonstrating the observed trends.

The results reveal the significant benefits of the TC-FCI calculation in terms of convergence and accuracy across a range of molecules. For instance, for the CO_2 molecule, the TC-FCI delivers atomization energies of 622.86 mH and 618.14 mH in the cc-pVDZ and cc-pVTZ basis sets, respectively. These values indicate a convergence towards highly accurate results, closely approxi-

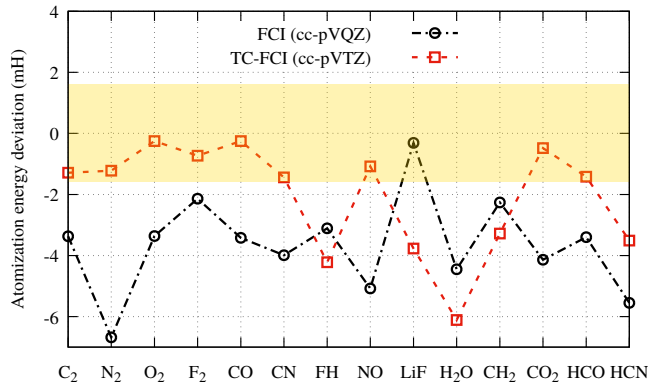


FIG. 6. Deviation of E_{FCI} and $E_{\text{TC-FCI}}$ from the estimated exact atomization energies (in mH) in cc-pVQZ and cc-pVTZ, respectively. The deviation of each method from the reference is defined using the convention $\delta E_{\text{method}} = E_{\text{method}} - E_{\text{estimated exact}}$. The figure includes a highlighted filled region, indicating the domain of chemical accuracy. Refer to Table III for the specific values.

imating the estimated exact value of 618.62 mH. Similarly, for O_2 , the TC-FCI provides atomization energies of 191.84 mH and 191.75 mH in the cc-pVDZ and cc-pVTZ basis sets, respectively. These values show remarkable alignment with the estimated exact value of 192.0 mH, further emphasizing the accuracy and convergence of the TC-FCI. In contrast, the conventional FCI calculation, even with the larger cc-pVQZ basis set, has difficulty converging to chemical accuracy for many molecules. This is evident in the results observed for various systems, such as C_2 , N_2 , and HCO , where the TC-FCI consistently surpasses the FCI in terms of accuracy and convergence, particularly in the modest cc-pVTZ basis set.

The TC-FCI/cc-pVTZ consistently outperforms the FCI/cc-pVQZ. However, in a few cases such as LiF (with 216.39 mH in the TC-FCI/cc-pVTZ versus 219.85 mH in the FCI/cc-pVQZ), the TC-FCI/cc-pVTZ does not exceed the efficiency of the FCI/cc-pVQZ. This observation could be ascribed to the use of a relatively simple correlation factor. Our future work will aim to explore the application of the TC-FCI with more sophisticated Jastrow factors to further enhance its performance and accuracy.

IV. CONCLUSION

In this work, we introduced the theoretical framework of SCI using a set of bi-orthogonal orbitals within the context of TC calculations. We employed a linearized version of a recently developed inexpensive three-body correlation factor [16](#), which eliminates the need for re-

optimizing the correlation factor for each molecule and facilitates an efficient analytical/numerical evaluation of the integrals required in TC calculations. After establishing the main equations, we explored various aspects of the current approach numerically. We first examined the benefits of using bi-orthogonal orbitals in TC calculations by studying the impact of the fc approximation on a set of IPs and AEs. Our findings indicate that the fc approximation has a similar impact in TC calculations using bi-orthogonal orbitals as in standard wavefunction techniques (typically a few 0.1 mH), while an order of magnitude greater variation is observed when using the RHF orbitals. These observations support the idea of conducting TC calculations using a bi-orthogonal framework, as the fc approximation is essential for handling large systems. We then investigated the convergence of the current BiO-TC-SCI framework compared to standard SCI approaches. Our results show that similar convergence can be expected, and that linear extrapolation is feasible, making our BiO-TC-SCI approach as robust as any standard SCI approach. We also examined the ability of the BiO-TC-SCI algorithm to handle strongly correlated systems by breaking the CO double bond, and demonstrated that the size consistency property is fulfilled. Finally, we assessed the quality of the current correlation factor on a set of 14 small organic molecules. Our results show that even with such a simple correlation factor, the accuracy is typically better than a standard quadruple zeta calculation. It is important to note that thanks to the specific form of the correlation factor used here, no optimization of the latter was needed for molecular calculations.

ACKNOWLEDGMENTS

This work was performed using HPC resources from GENCI-TGCC (gen1738,gen12363) and from CALMIP (Toulouse) under allocation P22001, and was also supported by the European Centre of Excellence in Exascale Computing TREX — Targeting Real Chemical Accuracy at the Exascale. This project has received funding from the European Union’s Horizon 2020 — Research and Innovation program — under grant agreement no. 952165. Emmanuel Giner would like to thank Julien Toulouse for fruitful discussions regarding the bi orthogonal basis sets.

- ¹S. F. Boys and N. C. Handy, *Proceedings of the Royal Society of London. A. Mathematical and Physical Sciences* **310**, 43 (1969).
- ²J. O. Hirschfelder, *The Journal of Chemical Physics* **39**, 3145 (1963).
- ³S. Ten-no, *Chemical Physics Letters* **330**, 169 (2000).
- ⁴E. Giner, *The Journal of Chemical Physics* **154**, 084119 (2021).
- ⁵S. F. Boys and N. C. Handy, *Proceedings of the Royal Society of London. A. Mathematical and Physical Sciences* **310**, 63 (1969).
- ⁶J. W. Moskowitz, K. E. Schmidt, M. A. Lee, and M. H. Kalos, *The Journal of Chemical Physics* **76**, 1064 (1982).
- ⁷K. E. Schmidt and J. W. Moskowitz, *The Journal of Chemical Physics* **93**, 4172 (1990).

TABLE III. Atomization energies (in mH) obtained using the standard extrapolated FCI or the extrapolated TC-FCI in different basis sets.

	CIPSI			TC-CIPSI		Estimated exact ⁸⁷
	cc-pVDZ	cc-pVTZ	cc-pVQZ	cc-pVDZ	cc-pVTZ	
C ₂	207.50	223.11	228.83	226.03	230.91	232.2
N ₂	319.13	345.72	356.02	359.67	361.48	362.7
O ₂	167.84	182.28	188.64	191.84	191.75	192.0
F ₂	44.38	56.39	60.06	58.18	61.47	62.2
CO	385.95	401.50	408.68	413.52	411.85	412.1
CN	254.40	274.40	283.21	282.24	285.76	287.2
FH	201.64	218.31	223.07	217.59	221.96	226.18
NO	211.60	229.88	237.67	242.32	241.67	242.75
LiF	196.06	211.84	219.85	210.15	216.39	220.16
H ₂ O	333.80	359.09	367.19	355.33	365.53	371.64
CH ₂ ^a	263.80	281.80	286.34	275.75	285.32	288.6
CO ₂	569.29	604.20	614.48	622.86	618.14	618.62
HCO	407.83	430.85	439.78	438.92	441.76	443.18
HCN	451.74	481.59	491.51	488.25	493.55	497.06

^a ¹A₁ state.

- ⁸C. J. Umrigar, K. G. Wilson, and J. W. Wilkins, *Phys. Rev. Lett.* **60**, 1719 (1988).
- ⁹J. W. Moskowitz and K. E. Schmidt, *The Journal of Chemical Physics* **97**, 3382 (1992).
- ¹⁰A. Mushinski and M. Nightingale, *The Journal of Chemical Physics* **101**, 8831 (1994).
- ¹¹C.-J. Huang, C. J. Umrigar, and M. P. Nightingale, *The Journal of Chemical Physics* **107**, 3007 (1997).
- ¹²A. D. Güçlü, G. S. Jeon, C. J. Umrigar, and J. K. Jain, *Phys. Rev. B* **72**, 205327 (2005).
- ¹³P. López Ríos, P. Seth, N. D. Drummond, and R. J. Needs, *Phys. Rev. E* **86**, 036703 (2012).
- ¹⁴B. M. Austin, D. Y. Zubarev, and W. A. J. Lester, *Chemical Reviews* **112**, 263 (2012).
- ¹⁵A. Lüchow, A. Sturm, C. Schulte, and K. Haghighi Mood, *The Journal of Chemical Physics* **142** (2015), 10.1063/1.4909554.
- ¹⁶A. Ammar, A. Scemama, and E. Giner, *arXiv* (2023), 10.48550/arXiv.2303.02436, 2303.02436.
- ¹⁷S. F. Boys and N. C. Handy, *Proceedings of the Royal Society of London. A. Mathematical and Physical Sciences* **309**, 209 (1969).
- ¹⁸S. F. Boys and N. C. Handy, *Proceedings of the Royal Society of London Series A* **311**, 309 (1969).
- ¹⁹N. C. Handy, *The Journal of Chemical Physics* **51**, 3205 (1969).
- ²⁰S. F. Boys, *Proceedings of the Royal Society of London. A. Mathematical and Physical Sciences* **309**, 195 (1969).
- ²¹N. C. Handy, *Molecular Physics* **21**, 817 (1971).
- ²²N. C. Handy, *Molecular Physics* **23**, 1 (1972).
- ²³E. A. G. Armour, *Molecular Physics* **24**, 181 (1972).
- ²⁴F. Bernardi and S. F. Boys, *Molecular Physics* **25**, 35 (1973).
- ²⁵F. Bernardi, *Journal de physique* **34**, 373 (1973).
- ²⁶E. A. G. Armour, *Chemical Physics Letters* **25**, 614 (1974).
- ²⁷N. Handy, in *Computational Techniques in Quantum Chemistry and Molecular Physics* (Springer, 1975) pp. 425–433.
- ²⁸J. P. Huggett and E. A. G. Armour, *Journal of Physics B: Atomic and Molecular Physics* **9**, 3263 (1976).
- ²⁹Dharma-wardana, M. W. C. and Grimaldi, François, *Phys. Rev. A* **13**, 1702 (1976).
- ³⁰P. N. Careless, D. Hyatt, and L. Stanton, *International Journal of Quantum Chemistry* **12**, 569 (1977).
- ³¹G. G. Hall and C. J. Miller, *Phys. Rev. A* **18**, 889 (1978).
- ³²W. R. Fimple and M. J. Unwin, *International Journal of Quantum Chemistry* **10**, 643 (1976).
- ³³O. Hino, Y. Tanimura, and S. Ten-no, *The Journal of Chemical Physics* **115**, 7865 (2001).
- ³⁴O. Hino, Y. Tanimura, and S. Ten-no, *Chemical Physics Letters* **353**, 317 (2002).
- ³⁵S. Ten-no and O. Hino, *International Journal of Molecular Sciences* **3**, 459 (2002).
- ³⁶S. Ten-no, *Chemical Physics Letters* **330**, 175 (2000).
- ³⁷A. J. Cohen, H. Luo, K. Guthier, W. Dobrautz, D. P. Tew, and A. Alavi, *The Journal of Chemical Physics* **151**, 061101 (2019).
- ³⁸K. Guthier, A. J. Cohen, H. Luo, and A. Alavi, *The Journal of Chemical Physics* **155**, 011102 (2021).
- ³⁹W. Dobrautz, A. J. Cohen, A. Alavi, and E. Giner, *The Journal of Chemical Physics* **156**, 234108 (2022).
- ⁴⁰T. Schraivogel, A. J. Cohen, A. Alavi, and D. Kats, *The Journal of Chemical Physics* **155**, 191101 (2021).
- ⁴¹T. Schraivogel, E. M. Christlmaier, P. L. Ríos, A. Alavi, and D. Kats, (2023).
- ⁴²A. Baiardi and M. Reiher, *The Journal of Chemical Physics* **153**, 164115 (2020).
- ⁴³A. Baiardi, M. Lesiuk, and M. Reiher, *J Chem Theory Comput* **18**, 4203 (2022).
- ⁴⁴Liao, Ke and Zhai, Huanchen and Christlmaier, Evelin Martine and Schraivogel, Thomas and Ríos, Pablo López and Kats, Daniel and Alavi, Ali, *Journal of Chemical Theory and Computation* **19**, 1734 (2023).
- ⁴⁵A. Ammar, E. Giner, and A. Scemama, *J Chem Theory Comput* **18**, 5325 (2022).
- ⁴⁶E. A. G. Armour, *Journal of Physics C: Solid State Physics* **13**, 343 (1980).
- ⁴⁷N. Umezawa and S. Tsuneyuki, *Phys. Rev. B* **69**, 165102 (2004).
- ⁴⁸R. Sakuma and S. Tsuneyuki, *Journal of the Physical Society of Japan* **75**, 103705 (2006).
- ⁴⁹S. Tsuneyuki, *Progress of Theoretical Physics Supplement* **176**, 134 (2008).
- ⁵⁰M. Ochi, K. Sodeyama, R. Sakuma, and S. Tsuneyuki, *The Journal of Chemical Physics* **136**, 094108 (2012).

- ⁵¹H. Luo, *The Journal of Chemical Physics* **136**, 224111 (2012).
- ⁵²M. Ochi and S. Tsuneyuki, *Journal of Physics: Conference Series* **454**, 012020 (2013).
- ⁵³M. Ochi, K. Sodeyama, and S. Tsuneyuki, *The Journal of Chemical Physics* **140**, 074112 (2014).
- ⁵⁴M. Ochi and S. Tsuneyuki, *Journal of Chemical Theory and Computation* **10**, 4098 (2014).
- ⁵⁵J. M. Wahlen-Strothman, C. A. Jiménez-Hoyos, T. M. Henderson, and G. E. Scuseria, *Phys. Rev. B* **91**, 041114 (2015).
- ⁵⁶M. Ochi and S. Tsuneyuki, *Chemical Physics Letters* **621**, 177 (2015).
- ⁵⁷M. Ochi, Y. Yamamoto, R. Arita, and S. Tsuneyuki, *The Journal of Chemical Physics* **144**, 104109 (2016).
- ⁵⁸P. Jeszenszki, H. Luo, A. Alavi, and J. Brand, *Phys. Rev. A* **98**, 053627 (2018).
- ⁵⁹H. Luo and A. Alavi, *Journal of Chemical Theory and Computation* **14**, 1403 (2018).
- ⁶⁰W. Dobrutz, H. Luo, and A. Alavi, *Phys. Rev. B* **99**, 075119 (2019).
- ⁶¹P. Jeszenszki, U. Ebling, H. Luo, A. Alavi, and J. Brand, *Phys. Rev. Res.* **2**, 043270 (2020).
- ⁶²K. Liao, T. Schraivogel, H. Luo, D. Kats, and A. Alavi, *Phys. Rev. Res.* **3**, 033072 (2021).
- ⁶³M. Ochi, R. Arita, and S. Tsuneyuki, *Phys. Rev. Lett.* **118**, 026402 (2017).
- ⁶⁴M. Ochi, *Comput Phys Commun*, 108687 (2023).
- ⁶⁵A. Ammar, A. Scemama, and E. Giner, *J Chem Phys* **157**, 134107 (2022).
- ⁶⁶A. A. Holmes, C. J. Umrigar, and S. Sharma, *J. Chem. Phys.* **147**, 164111 (2017).
- ⁶⁷J. E. T. Smith, B. Mussard, A. A. Holmes, and S. Sharma, *J Chem Theory Comput* **13**, 5468 (2017).
- ⁶⁸Y. Yao and C. J. Umrigar, *J Chem Theory Comput* **17**, 4183 (2021).
- ⁶⁹J. W. Park, *J Chem Theory Comput* **17**, 1522 (2021).
- ⁷⁰Y. Guo, N. Zhang, Y. Lei, and W. Liu, *J Chem Theory Comput* **17**, 7545 (2021).
- ⁷¹P.-F. Loos, A. Scemama, A. Blondel, Y. Garniron, M. Caffarel, and D. Jacquemin, *J Chem Theory Comput* **14**, 4360 (2018).
- ⁷²P.-F. Loos, F. Lipparini, M. Boggio-Pasqua, A. Scemama, and D. Jacquemin, *J Chem Theory Comput* **16**, 1711 (2020).
- ⁷³M. Moshinsky and T. Seligman, *Annals of Physics* **66**, 311 (1971).
- ⁷⁴J. F. Gouyet, *International Journal of Quantum Chemistry* **7**, 139 (1973).
- ⁷⁵J. P. Dahl, *International Journal of Quantum Chemistry* **14**, 191 (1978).
- ⁷⁶P. W. Payne, *The Journal of Chemical Physics* **77**, 5630 (1982).
- ⁷⁷Péter R. Surján, *Second Quantized Approach to Quantum Chemistry. An Elementary Introduction* (Springer Berlin, Heidelberg, 2011).
- ⁷⁸F. Takano, *Journal of the Physical Society of Japan* **14**, 348 (1959).
- ⁷⁹A. A. Cantu, D. J. Klein, F. A. Matsen, and T. H. Seligman, *Theoretica chimica acta* **38**, 341 (1975).
- ⁸⁰Vladimír Kvasnička, *Chemical Physics Letters* **51**, 165 (1977).
- ⁸¹M. Kojo and K. Hirose, *Journal of Computational and Theoretical Nanoscience* **6**, 2567 (2009).
- ⁸²P. S. Epstein, *Phys. Rev.* **28**, 695 (1926).
- ⁸³R. K. Nesbet, *Proc. R. Soc. A* **230**, 312 (1955).
- ⁸⁴K. Hirao and H. Nakatsuji, *J Comput Phys* **45**, 246 (1982).
- ⁸⁵Y. Garniron, A. Scemama, P.-F. Loos, and M. Caffarel, *J Chem Phys* **147**, 034101 (2017).
- ⁸⁶Y. Garniron, K. Gasperich, T. Applencourt, A. Benali, A. Ferté, J. Paquier, B. Pradines, R. Assaraf, P. Reinhardt, J. Toulouse, P. Barbaresco, N. Renon, G. David, J. P. Malrieu, M. Vénil, M. Caffarel, P. F. Loos, E. Giner, and A. Scemama, *J. Chem. Theory Comput.* **15**, 3591 (2019).
- ⁸⁷Y. Yao, E. Giner, J. Li, J. Toulouse, and C. J. Umrigar, *The Journal of Chemical Physics* **153** (2020), 10.1063/5.0018577, 124117.